ARTICLES

Journal of Semiconductors
(2021) 42, 122902
doi: 10.1088/1674-4926/42/12/122902

Electrical transport properties of cerium doped Bi_2Te_3 thin films grown by molecular beam epitaxy

Peng Teng[1, 2, 3, ‡], Tong Zhou[4, ‡], Yonghuan Wang[2, 3], Ke Zhao[1, †], Xiegang Zhu[2, 3, †], and Xinchun Lai[2]

[1]Southwest Jiaotong University, School of Physical Science and Technology, Chengdu 610031, China

[2]Science and Technology on Surface Physics and Chemistry Laboratory, Jiangyou 621908, China

[3]Institute of Materials, China Academy of Engineering Physics, Mianyang 621700, China

[4]Beijing Institute for Advanced Study, National University of Defense Technology, Beijing 100020, China

Abstract: Introducing magnetism into topological insulators (TIs) can tune the topological surface states and produce exotic physical effects. Rare earth elements are considered as important dopant candidates, due to their large magnetic moments from heavily shielded 4f electrons. As the first element with just one 4f electron, cerium (Ce) offers an ideal platform for exploring the doping effect of f-electron in TIs. Here in this work, we have grown cerium-doped topological insulator Bi_2Te_3 thin films on an Al_2O_3(0001) substrate by molecular beam epitaxy (MBE). Electronic transport measurements revealed the Kondo effect, weak anti-localization (WAL) effect and suppression of surface conducting channels by Ce doping. Our research shows the fundamental doping effects of Ce in Bi_2Te_3 thin films, and demonstrates that such a system could be a good platform for further research.

Key words: topological insulators; molecular beam epitaxy; Kondo effect; weak anti-localization effect

Citation: P Teng, T Zhou, Y H Wang, K Zhao, X G Zhu, and X C Lai, Electrical transport properties of cerium doped Bi_2Te_3 thin films grown by molecular beam epitaxy[J]. *J. Semicond.*, 2021, 42(12), 122902. http://doi.org/10.1088/1674-4926/42/12/122902

1. Introduction

Topological insulators (TIs) are a class of materials with special topological features in energy bands. Due to the topological surface states protected by time reversal symmetry (TRS)[1–3], three-dimensional topological insulators (3D-TIs), such as Bi_2Se_3[1, 4], Bi_2Te_3[5] and Sb_2Te_3[6] have attracted great attention in the past few decades. TRS can be broken by introducing magnetism, which could unlock many exotic physical phenomena, such as quantum anomalous Hall effect (QAHE)[7], topological magnetoelectric effect[8] and mirror magnetic monopole[9], *etc.* The method of doping magnetic elements was widely adopted to introduce magnetism into TIs. Conventionally, transition elements (such as Mn, Fe, V, Co, Cr, *etc.*[10–20]) were used as dopants to study the doping effect of d electrons in TIs, among which the discovery of QAHE in Cr-doped $Cr_{0.15}(Bi_{0.1}Sb_{0.9})_{1.85}Te_3$ thin films was well noted[10]. It should be stressed that the typical dopant concentration of transition elements was considerably high (from ~ 0.03 to 0.075 at.), which might complicate the structural phases and chemical homogeneity of the pristine topological materials. What is more, extremely low temperature environment, *i.e.*, in the range of sub-kelvin, was needed for the interplay between magnetism and topological states taking effects.

Compared with transition elements, rare earth (RE) elements could be optional dopant candidates for the following reasons. On one hand, they usually possess larger local magnetic moments than transition elements, which implies the possibility of larger interactions between local magnetic moments from 4f electrons with topological states, and might result in reducing the dopant concentration to achieve the desired strength of magnetic interactions. On the other hand, the trivalent state of RE ions can substitute the trivalent Bi/Sb ions in TIs without changing the charge carrier density[21]. Research on doping TIs with various rare earth elements (such as Ce, Sm, Eu, Gd, etc.[22–26]) have been reported, and strong competition between anti-ferromagnetism and topological states was observed. Among all the RE elements, the isolated Ce atom has only one f electron, and it is ionized into the trivalent state (Ce^{3+}) when diluted doped into other materials. This implies that Ce doped topological insulators might serve as a prototypical platform to study the interactions between f-electron and topological states and explore possible exotic physical phenomena.

In this work, we reported the electronic transport properties of Ce-doped Bi_2Te_3 thin films grown on Al_2O_3(0001) substrate by molecular beam epitaxy (MBE) with various Ce concentrations. X-ray diffraction (XRD) revealed that Ce atoms substituted the Bi sites, resulting in the chemical formula of $(Ce_xBi_{1-x})_2Te_3$. Electronic transport measurements demonstrated Kondo effect and Fermi liquid behavior of $(Ce_xBi_{1-x})_2Te_3$ at low temperature. Weak anti-localization (WAL) effect that is closely related to the topological properties of TIs is experimentally investigated by magnetic transport measurements and theoretically studied by using the Hikami–Larkin–Nagaoka (HLN) model[27]. Our analysis showed that the surface conducting channels persisted to be two for x in the range from 0 to 0.02, and the conducting ability is suppressed as Ce concentration further increased, indicating

Peng Teng and Tong Zhou have contributed equally to this paper.
Correspondence to: K Zhao, zhaoke@swjtu.edu.cn; X G Zhu, zhuxiegang@caep.cn
Received 26 MAY 2021; Revised 31 MAY 2021.

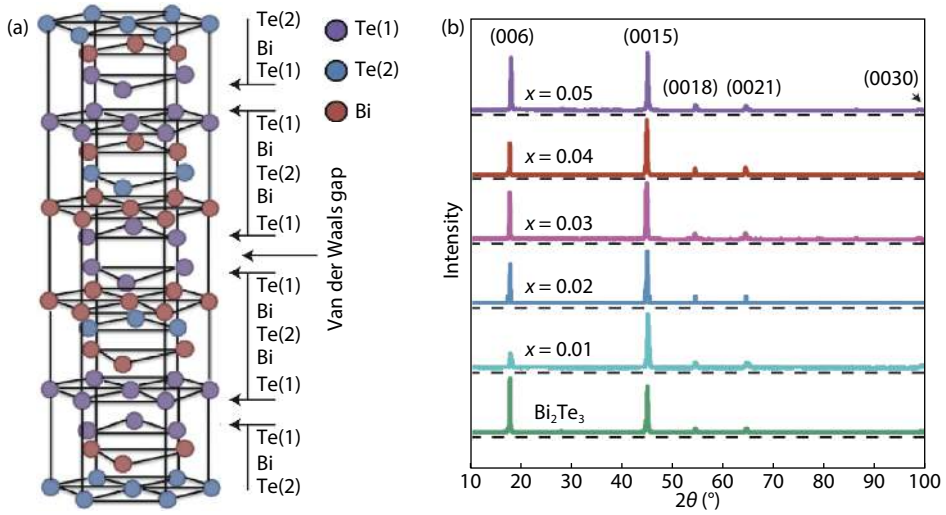

Fig. 1. (Color online) (a) Schematic crystal structure of Bi_2Te_3. (b) XRD patterns of $(Ce_xBi_{1-x})_2Te_3$ thin films (x = 0, 0.01, 0.02, 0.03, 0.04, 0.05).

the possible competition between magnetic order and topological states.

2. Experimental methods

Pristine and Ce-doped Bi_2Te_3 thin films were grown on an Al_2O_3(0001) substrate by MBE, following the well-established three temperature methods[28]. The base pressure of the MBE chamber was better than 1×10^{-10} mbar and rose to less than 5×10^{-10} mbar during the growth. Standard Knudsen cells were used to evaporate Ce(3N), Bi(5N) and Te(5N) sources. The flux rates of the sources were calibrated by *in-situ* quartz crystal microbalance (QCM). Ce doping was realized by co-evaporating Ce during the MBE growth of Bi_2Te_3 thin films, and its concentration was carefully tuned by finely adjusting the evaporating temperature of the Ce source. During the growth, Bi and Te sources were kept at 530 and 315 °C, corresponding to flux rate of 0.199 and 0.779 Å/s, respectively. The Ce source was kept at 1280, 1310, 1340, 1360, and 1370 °C, to grow $(Ce_xBi_{1-x})_2Te_3$ thin films with various Ce concentration (x = 0, 0.01, 0.02, 0.03, 0.04, 0.05, respectively). *ex-situ* X-ray diffraction (XRD) measurements were performed to characterize the out-of-plane lattice parameters. Transport measurements were performed with the standard four-probe method by a physical property measurement system (Quantum Design PPMS-9). High purity Indium (5N) was used as electrode contacts.

3. Results and discussions

Fig. 1(a) shows the crystal structure of Bi_2Te_3. Bi_2Te_3 has a layered hexagonal structure. The smallest repeating unit consists of five atomic layers with a stacking sequence of -Te(1)-Bi-Te(2)-Bi-Te(1)-, which is called a quintuple layer (QL). The interaction between neighboring QLs is the relatively weak van der Waals interaction. The thickness of all the samples was kept at 100 QLs, *i.e.*, about 100 nm. Fig. 1(b) shows the XRD results of the $(Ce_xBi_{1-x})_2Te_3$ samples, where only the (00L) peaks of Bi_2Te_3 are present in the spectra. The absence of other diffraction peaks in the XRD suggests that the sample surface is well oriented in the direction parallel to the (0001) plane of Bi_2Te_3. The lattice parameters c perpendicular to the sample surface for all the samples were calculated. All the c values disperse within 3.045 ± 0.007 nm for all the samples, where 3.045 nm corresponds to the lattice parameter of the pristine Bi_2Te_3 thin film. This means that the differences of c between the Ce-doped and pristine Bi_2Te_3 thin films are less than ~ 0.2 %, indicating that Ce has substituted Bi during the growth, which is consistent with the substitutional doping scenario with the RE^{3+} ion iso-electronically substituting for Bi^{3+}[21].

Transport measurements were performed above 3.4 K (the onset superconducting transition temperature of indium, which was used as electrode contacts) to eliminate the influence of the superconducting effects from indium. The curves of the longitudinal resistivity versus temperature ($\rho_{xx}(T)$) for the pristine and doped thin films are shown in Fig. 2(a), where all the curves are normalized with the resistivity at 300 K and are shifted vertically for a better view. The $\rho_{xx}(T)$ curve for the pristine Bi_2Te_3 thin film is consistent with the results from the literature[29], demonstrating metallic behavior from RT to the lowest temperature, which is resulted from the fact that the electronic properties of Bi_2Te_3 bulk or thin film are usually dominated by intrinsic n-type and/or p-type carriers[6, 30]. The discrepancy from metallic behavior at low temperature (from 3.5 to 25 K) in $\rho_{xx}(T)$ occurred as cerium was doped into Bi_2Te_3, as shown in Fig. 2(b), *i.e.*, resistivity minimum developed with Ce doping. Due to the large local magnetic moments of diluted Ce^{3+} ions in Bi_2Te_3, Kondo effect[31] would be a straightforward explanation of the occurrence of resistivity minimum at a low temperature, which contributed an increasing logarithmic term in resistivity as temperature decreased. In order to simulate the resistivity behaviors at low temperature, the following expression was used to fit the normalized (with the resistivity at 25 K being set to 1) experimental $\rho_{xx}(T)$ curves between 3.5 and 25 K:

$$\rho_{xx} = \rho_0 + AT^2 - B\log T, \tag{1}$$

where ρ_0 is the residual resistivity, AT^2 and $-B\log T$ represent contributions from Fermi liquid behavior and Kondo effect at low temperature, respectively. For pristine Bi_2Te_3, considering there would be no Kondo effect, the last term was set to be zero. The fitted parameters ρ_0, A and B are listed in Table 1, and the corresponding $\rho - T$ relationships are

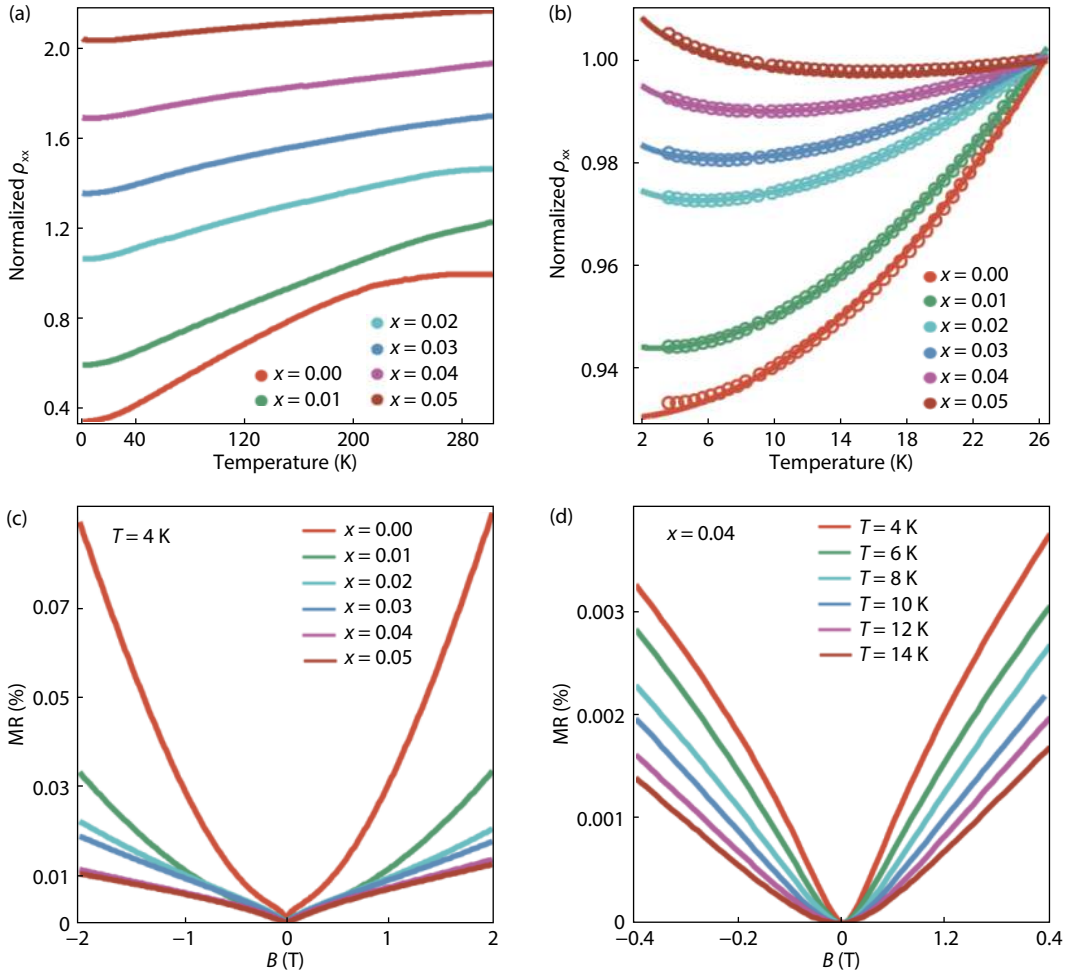

Fig. 2. (Color online) (a) Resistivity of $(Ce_xBi_{1-x})_2Te_3$ samples at different temperatures. Curves have been shifted for better visibility. (b) Normalized resistivity of $(Ce_xBi_{1-x})_2Te_3$ at 3.5–25 K. (Solid lines: fits to Eq. (1).) (c) Magnetoresistance of $(Ce_xBi_{1-x})_2Te_3$ at 4 K. (d) Magnetoresistance of $(Ce_{0.04}Bi_{0.96})_2Te_3$ at 4–14 K.

Table 1. Fitting results of the parameters in Eq. (1). All parameters are in corresponding SI units.

Samples	ρ_0	A (10^{-5})	B (10^{-3})
$x = 0$	0.9303	10.59	–
$x = 0.01$	0.945	9.39	1.607
$x = 0.02$	0.9766	5.258	3.193
$x = 0.03$	0.9858	4.053	3.62
$x = 0.04$	0.9981	2.633	4.632
$x = 0.05$	1.013	1.439	7.004

demonstrated as solid curves in Fig. 2(b).

As shown in Table 1, as the dopant concentration increases, the Fermi liquid behavior and the Kondo effect compete with each other, indicated by the gradual decrease of A and increase of B. In general, the low temperature transport behavior of $(Ce_xBi_{1-x})_2Te_3$ films is mainly determined by the Kondo effect of Ce and the Fermi liquid behavior of electrons. The more the dopant, the stronger the Kondo effect and the weaker the Fermi liquid behavior.

Figs. 2(c) and 2(d) show the evolution of normalized magnetoresistance (MR) with Ce concentration x and temperature for $x = 0.04$, respectively, with MR being defined as:

$$\mathrm{MR} = \frac{R(B) - R(0)}{R(0)} \times 100\%, \tag{2}$$

where $R(B)$ is the resistance measured under magnetic field B, $R(0)$ is the resistance measured under zero field. Similar to the previous report[32], all samples have very low MR. WAL is a destructive quantum interference effect caused by two electron scattering trajectories protected by time reversal symmetry, which stems from the π berry phase[33]. Fig. 2(c) shows that the magnetoresistance near zero field increases rapidly with increasing field, and then gradually increases linearly under high field. This trend of magnetoresistance is a distinctive feature of weak anti-localization (WAL)[33], and WAL is gradually suppressed as the dopant concentration increases. It implies the possibilities that the introduced Ce impurity destroys the time reversal invariant symmetry which is crucial to the topological properties of the pristine Bi_2Te_3 thin film.

The effect of WAL in MR can be described by the HLN model[27]. Figs. 3(a) and 3(b) show the magnetic conductance of samples with different concentration. For an ideal TI surface, the change of conductance under field B can be expressed as:

$$\Delta G_{xx}(B) \equiv G(B) - G(0) \cong \alpha \frac{e^2}{2\pi^2\hbar}\left[\psi\left(\frac{1}{2} + \frac{B_\phi}{B}\right) - \ln\left(\frac{B_\phi}{B}\right)\right], \tag{3}$$

where $G(B)$ is magnetoconductance, e is the electronic charge, $\hbar$ is the reduced Planck constant, ψ is the digamma function and B_ϕ is a characteristic magnetic field expressed as

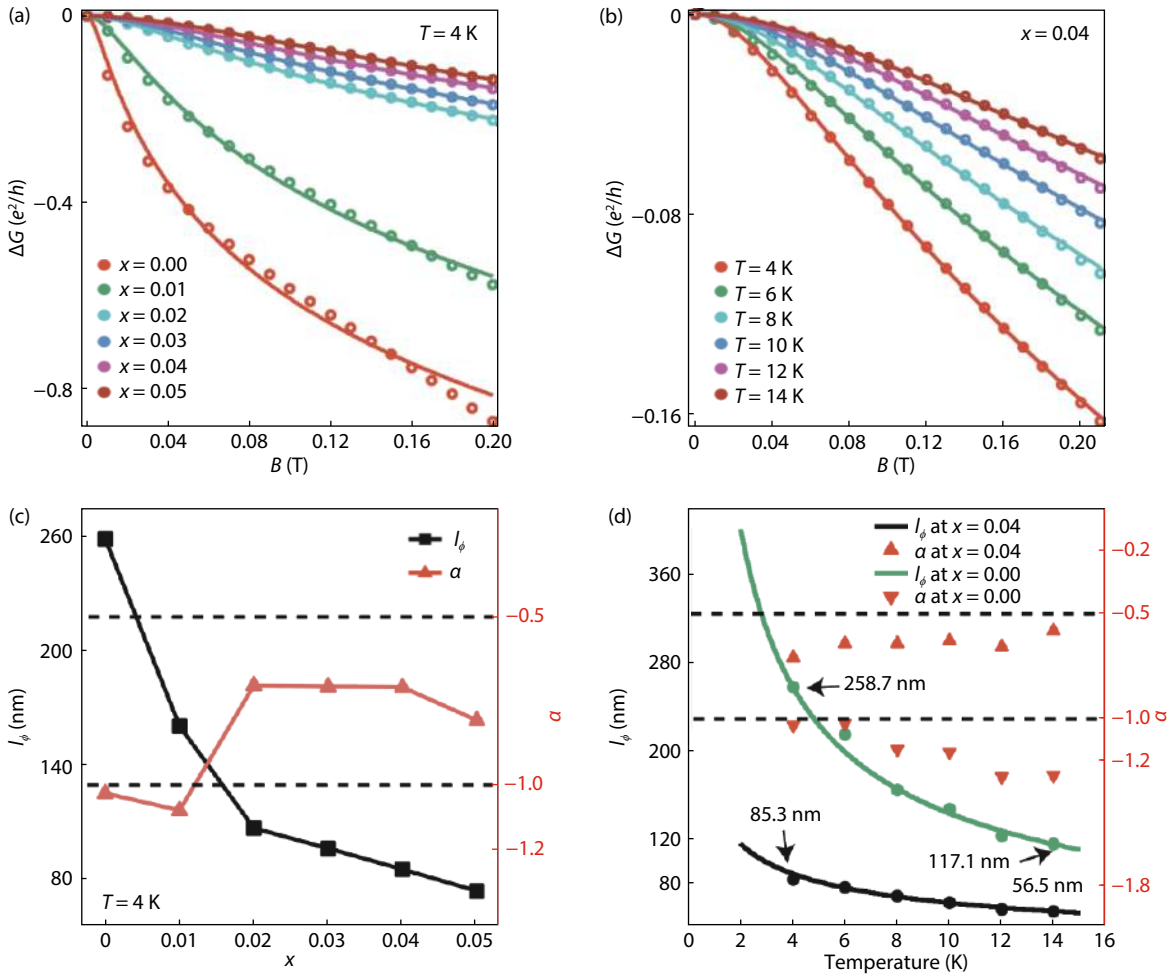

Fig. 3. (Color online) (a) Magnetoconductance of samples with different dopant concentrations under different perpendicular magnetic field at 4 K (solid lines – fits to Eq. (3)). (b) Magnetoconductance of $(Ce_{0.04}Bi_{0.96})_2Te_3$ under different perpendicular magnetic field at different temperatures (solid lines – fits to Eq. (3)). (c) The change of fitting parameters l_ϕ and α with different dopant concentration. (d) The change of fitting parameters l_ϕ and α of $(Ce_{0.04}Bi_{0.96})_2Te_3$ and Bi_2Te_3 at different temperatures (solid line – fit to Eq. (5)).

Table 2. Parameters extracted by fitting magnetoconductance data with Eqs. (3) and (5). l_ϕ is the phase coherence length, α is the coefficient in HLN formula and m is the power factor in Eq. (5).

$(Ce_xBi_{1-x})_2Te_3$	$x = 0$	$x = 0.01$	$x = 0.02$	$x = 0.03$	$x = 0.04$	$x = 0.05$
l_ϕ at 4 K (nm)	258.7	160.5	107	96.3	85.3	73.9
l_ϕ at 14 K (nm)	117.1	80.3	61.9	56.3	56.5	52.0
α at 4 K	−1.027	−1.079	−0.704	−0.708	−0.709	−0.809
α at 14 K	−1.266	−1.119	−0.719	−0.708	−0.580	−0.601
m	−0.633	−0.5624	−0.415	−0.411	−0.378	−0.306

$B_\phi = \hbar/4el_\phi^2$, where l_ϕ is the phase coherence length. As demonstrated in Figs. 3(a) and 3(b), all experimental conductance data can be fitted well by the HLN formula. The coefficient α and l_ϕ are extracted by fitting the HLN model, and the results are listed in Table 2 and also shown in Figs. 3(c) and 3(d). The fitting results show that l_ϕ gradually decreases with increasing concentration and temperature. This effect is expected because the dopant introduces disorder and magnetism to the system. The value of α is between −0.6 and −1, similar to the results of Yu *et al.*[34]. And the α can be further expressed by:

$$\alpha = N\alpha, \tag{4}$$

where α should be −0.5 for the topological surface states of symplectic universality class, and N is the number of independent conducting channels[27]. The relatively large values of N and α may be caused by the thick film's 3D WAL effect and multiple effective surfaces[32]. The fitting results show that the number of conducting channels is about 2 for $x = 0$, and it still maintains the same state for $x = 0.01$. However, the surface conducting channels are reduced for $x > 0.01$. It may indicate that the transportation ability of topological surface states has been suppressed for $x > 0.01$, which suggests there is a strong competition between magnetic order and the topological surface states for $x = 0.01$–0.02. The change of N and α in the doped samples suggested that Ce may have brought certain magnetic order into the TI film, partially suppressing the topological surface states while not creating any additional bulk conducting channel in the body state. The relation

between l_ϕ and temperature can be expressed by a power law[35]:

$$l_\phi = AT^m, \quad (5)$$

where T is the temperature and the factor m is related to the type of dominant mechanism of WAL. It is reported that for two-dimensional e–e scattering, the power law dependence should be $T^{-0.5}$; while for three-dimensional scattering, it is $T^{-0.75}$[36, 37]. Here, the value of m is between –0.3 and –0.6. This further confirms that the WAL effect is still dominated by the two-dimensional Nyquist e–e interaction though the TSSs is partially suppressed by the dopants Ce.

4. Conclusions

$(Ce_xBi_{1-x})_2Te_3$ (x = 0, 0.01, 0.02, 0.03, 0.04, 0.05) monocrystalline films with a thickness of 100 nm were successfully grown on sapphire substrates by MBE, and the electrical transport properties have been investigated. The resistivity shows metallic behavior at $T > 25$ K and semiconductor behavior when between 5–25 K. This resistivity behavior at low temperature is mainly due to the Kondo effect of Ce and the Fermi liquid behavior of electrons, which are confirmed by Kondo theory fitting. The contribution of Kondo effect increases with increasing Ce concentration, while the contribution of Fermi liquid decreases. Besides, WAL effect was also observed from the magnetoresistance and magnetoconductance. From the fitting of the HLN model, we confirm that the WAL effect is mainly dominated by the two-dimensional Nyquist e-e interaction. The phase coherence length and the number of conducting channels extracted from HLN fitting decrease as the concentration increases, which indicates a higher concentration of dopant may further suppress or even damage the topological properties of the TI. This indicates that there is a strong competition between the topological surface states and the magnetic order introduced by dopant Ce. Through doping Ce, this work successfully introduces RE elements into topological materials and preliminary investigates its influence on the transportation properties. It may lay the foundation for further research on the influences of RE elements on topological materials, which may open the door to the study of exotic physical properties, such as QAHE of TIs at elevated temperatures.

Acknowledgements

This work was supported by the Key Research and Development Program of China (No. 2017YFA0303104), the SPC-Lab Research Fund (No. WDZC201901) and the National Science Foundation of China (No. U1630248).

References

[1] Zhang H J, Liu C X, Qi X L, et al. Topological insulators in Bi_2Se_3, Bi_2Te_3, and Sb_2Te_3 with a single Dirac cone on the surface. Nat Phys, 2009, 5, 438
[2] Teo J, Fu L, Kane C L. Surface states and topological invariants in three-dimensional topological insulators: Application to $Bi_{1-x}Sb_x$. Phys Rev B, 2008, 78, 045426
[3] Fu L, Kane C L. Topological insulators with inversion symmetry. Phys Rev B, 2007, 76, 045302
[4] Xia Y, Qian D, Hsieh D, et al. Observation of a large-gap topological-insulator class with a single Dirac cone on the surface. Nat Phys, 2009, 5, 398
[5] Chen Y L, Analytis J G, Chu J H, et al. Experimental realization of a three-dimensional topological insulator Bi_2Te_3. Science, 2009, 325, 178
[6] Hsieh D, Xia Y, Qian D, et al. Observation of time-reversal-protected single-cone topological insulator states in Bi_2Te_3 and Sb_2Te_3. Phys Rev Lett, 2009, 103, 146401
[7] Yu R, Zhang W, Zhang H J, et al. Quantized anomalous Hall effect in magnetic topological insulators. Science, 2010, 329, 61
[8] Essin A M, Moore J E, Vanderbilt D. Magnetoelectric polarizability and axion electrodynamics in crystalline insulators. Phys Rev Lett, 2009, 102, 146805
[9] Qi X L, Li R, Zang J, et al. Inducing a magnetic monopole with topological surface states. Science, 2009, 323, 1184
[10] Chang C Z, Zhang J, Feng X, et al. Experimental observation of the quantum anomalous Hall effect in a magnetic topological insulator. Science, 2013, 340, 167
[11] Collins-McIntyre L J, Watson M D, Baker A A, et al. X-ray magnetic spectroscopy of MBE-grown Mn-doped Bi_2Se_3 thin films. AIP Adv, 2014, 4, 127136
[12] Liu W, West D, He L, et al. Atomic-scale magnetism of Cr-doped Bi_2Se_3 thin film topological insulators. ACS Nano, 2015, 9, 10
[13] Li M, Chang C Z, Wu L, et al. Experimental verification of the van Vleck nature of long-range ferromagnetic order in the vanadium-doped three-dimensional topological insulator Sb_2Te_3. Phys Rev Lett, 2015, 114, 146802
[14] Fan Y, Kou X, Upadhyaya P, et al. Electric-field control of spin–orbit torque in a magnetically doped topological insulator. Nat Nanotechnol, 2016, 11, 352
[15] J Teng, N Liu, Y Q Li. Mn-doped topological insulators: a review. J Semicond, 2019, 40(8), 081507
[16] Kou X, Pan L, Wang J, et al. Metal-to-insulator switching in quantum anomalous Hall states. Nat Commun, 2015, 6, 8474
[17] Liang J, Yao X, Zhang Y J, et al. Formation of Fe-Te nanostructures during in situ Fe heavy doping of Bi_2Te_3. Nanomaterials, 2019, 9(5), 782
[18] Zimmermann S, Steckel F, Hess C, et al. Spin dynamics and magnetic interactions of Mn dopants in the topological insulator Bi_2Te_3. Phys Rev B, 2016, 94, 125205
[19] Wang H L, Ma J L, Wei Q Q, et al. Mn doping effects on the gate-tunable transport properties of Cd_3As_2 films epitaxied on GaAs. J Semicond, 2020, 41(7), 072903
[20] Dietl T, Bonanni A, Ohno H. Families of magnetic semiconductors - an overview. J Semicond., 2019, 40(8), 080301
[21] Hesjedal T. Rare earth doping of topological insulators: A brief review of thin film and heterostructure systems. Phys Status Solidi A, 2019, 216, 1800726
[22] Kim S W, Kim H, Kim J K, et al. Effect of antiferromagnetic order on topological electronic structure in Eu-substituted Bi_2Se_3 single crystals. APL Mater, 2020, 8, 111108
[23] Yue Z, Zhao W, Cortie D, et al. Modulation of crystal and electronic structures in topological insulators by rare-earth doping. ACS Appl Electron Mater, 2019, 1(9), 1929
[24] Kim J, Lee K, Takabatake T, et al. Magnetic transition to antiferromagnetic phase in gadolinium substituted topological insulator Bi_2Te_3. Sci Rep, 2015, 5, 10309
[25] Kim S W, Vrtnik S, Dolinše J, et al. Antiferromagnetic order induced by gadolinium substitution in Bi_2Se_3 single crystals. Appl Phys Lett, 2015, 106, 252401
[26] Lee H S, Kim J, Lee K, et al. Study of Ho-doped Bi_2Te_3 topological insulator thin films. Appl Phys Lett, 2015, 107, 182409
[27] Hikami S, Larkin A I, and Nagaoka Y. Spin-orbit interaction and magnetoresistance in the two dimensional random system. Prog Theor Phys, 1980, 63, 707
[28] Li Y Y, Wang G, Zhu X G, et al. Intrinsic topological insulator Bi_2Te_3 thin films on Si and their thickness limit. Adv Mater, 2010, 22(36), 4002

[29] Hoefer K, Becker C, Rata D, et al. Intrinsic conduction through topological surface states of insulating Bi_2Te_3 epitaxial thin films. PNAS, 2014, 111(42), 14979
[30] Wang G, Zhu X G, Sun Y Y, et al. Topological insulator thin films of Bi_2Te_3 with controlled electronic structure. Adv Mater, 2011, 23, 2929
[31] Kondo J. Resistance minimum in dilute magnetic alloys. Prog Theor Phys, 1964, 32, 37
[32] He H T, Wang G, Zhang T, et al. Impurity effect on weak antilocalization in the topological insulator Bi_2Te_3. Phys Rev Lett, 2011, 106, 166805
[33] Lu H Z, Shen S Q. Weak localization and weak anti-localization in topological insulators. Spintronics VII, 2014, 9167, 91672E
[34] Kuntsevich A Y, Gabdullin A A, Prudkogliad V A, et al. Low-temperature Hall effect in bismuth chalcogenides thin films. Phys Rev B, 2016, 94, 235401
[35] Bao L, He L, Meyer N, et al. Weak anti-localization and quantum oscillations of surface states in topological insulator Bi_2Se_2Te. Sci Rep, 2012, 2, 726
[36] Cha J J, Kong D S, Hong S S, et al. Weak antilocalization in $Bi_2(Se_xTe_{1-x})_3$ nanoribbons and nanoplates. Nano Lett, 2012, 12, 1107
[37] Gilbertson A M, Newaz A K M, Chang W J, et al. Dimensional crossover and weak localization in a 90 nm n-GaAs thin film. Appl Phys Lett, 2009, 95, 012113

Peng Teng is a third-year graduate student majoring in optics at Southwest Jiaotong University. During the master's degree, he was engaged in the growth and characterization of topological insulator materials in the Institute of Materials Research, China Academy of Engineering Physics, by way of joint training.

Tong Zhou received his PhD degree in Electronic Science and Technology from the National University of Defense Technology in 2019. He is currently an associate professor at Beijing Institute for Advanced Study, National University of Defense Technology. His research interests include topological materials and their growth and electronic structure characterization.

Xiegang Zhu received his BS degree in Physics from Tsinghua University in 2006 and received his PhD degree in Physics from Tsinghua University in 2014. He is currently an associate professor at the Institute of Materials, China Academy of Engineering Physics. His research interests include topological insulators, f electron metals, heavy Fermion systems and their MBE growth and electronic structure characterization.